Published in final edited form as:
Atmos Pollut Res. 2021 ; 12(1): 148–158. doi:10.1016/j.apr.2020.08.030.

Gaseous Oxidized Mercury Dry Deposition Measurements in the Four Corners Area, U.S.A., after Large Power Plant Mercury Emission Reductions

Mark E. Sather,
Air Monitoring & Grants Section, U.S. Environmental Protection Agency (EPA) Region 6, 1201 Elm Street, Dallas, Texas 75270

Shaibal Mukerjee,
Center for Environmental Measurement and Modeling, U.S. EPA (E205-03), Research Triangle Park, North Carolina 27711

Luther Smith,
Serco, Inc., 4819 Emperor Blvd., Suite 400, Durham, North Carolina 27703

Johnson Mathew,
Houston Laboratory, U.S. EPA Region 6, 10625 Fallstone Road, Houston, Texas 77099

Clarence Jackson,
Houston Laboratory, U.S. EPA Region 6, 10625 Fallstone Road, Houston, Texas 77099

Michael Flournoy
Eurofins Frontier Global Sciences, 5755 8th St. E, Tacoma, Washington 98424

Abstract

Gaseous oxidized mercury (GOM) dry deposition measurements using surrogate surface passive samplers were collected at six sites in the Four Corners area, U.S.A., for the two-year period August, 2017-August, 2019, after the implementation of large power plant mercury emission reductions across the U.S.A. Two-year baseline GOM dry deposition measurements at the same six sites in the Four Corners area, taken before the implementation of U.S.A. power plant mercury control regulations, were conducted earlier from August, 2009-August, 2011. The GOM dry deposition rate estimate decreased at the Four Corners area high elevation remote mountain site of Molas Pass, Colorado (3249 m asl) from 0.4 ng/m^{2}h for August, 2009-August, 2011 to 0.3 ng/m^{2}h

Correspondence to: Mark E. Sather.

Supporting Material Available

Comparison of ICE-450 and Mustang S filter membranes at site NM95 (Figure S1); GOM Dry Deposition data time series at all 6 Four Corners area sites for August, 2017-August, 2019 (Figure S2); Back Trajectory Analysis at Mesa Verde National Park site (CO99) May 22 – June 5, 2018 (Figure S3); Back Trajectory Analysis at Mesa Verde National Park site (CO99) May 9 – May 22, 2018 (Figure S4); Back Trajectory Analysis at Mesa Verde National Park site (CO99) August 2 – August 15, 2017 (Figure S5); Back Trajectory Analysis at Mesa Verde National Park site (CO99) December 18, 2018 – January 1, 2019 (Figure S6); Back Trajectory Analysis at Mesa Verde National Park site (CO99) January 1 – January 15, 2019 (Figure S7); Mercury Wet Deposition Time Series 2009-2019 at Site CO99 (Figure S8); Mercury Wet Deposition Time Series 2009-2019 at Site CO96 (Figure S9); Dry deposition summary statistics (Table S1); Site-to-site comparisons of median values within the 2009-2011 and 2017-2019 sampling periods (Table S2); Within site seasonal comparisons for median values between spring/summer and fall/winter seasons (Table S3); Within site comparisons of median values between the 2017-2018 and 2018-2019 sampling for GOM dry, wet, and total deposition (Table S4).

for August, 2017-August, 2019. In contrast, GOM dry deposition rate estimates for the remaining five sites increased for August, 2017-August, 2019, ranging from 0.8-1.3 ng/m^2h, up from the August, 2009-August, 2011 range of 0.6-1.0 ng/m^2h. Comparisons of median GOM dry deposition values showed a statistically significant decrease of 17 ng/m^2 at the Molas Pass site between August, 2009-August, 2011 and August, 2017-August, 2019, and a statistically significant increase of 66 ng/m^2 and 64 ng/m^2, respectively, at the Mesa Verde National Park and Farmington Substation sites between August, 2009-August, 2011 and August, 2017-August, 2019. For the four years of GOM dry deposition data collected in the Four Corners area annual GOM dry deposition levels ranged from 2237 ng/m^2yr (at the Molas Pass high elevation remote mountain site) to 11542 ng/m^2yr (at the Mesa Verde National Park site), and the estimates were generally higher in magnitude in the spring and summer compared to the fall and winter. In light of the unexpected increases in GOM dry deposition rates at the non-remote sites, it is suggested that large regional wildfires and local anthropogenic mercury emission sources from cities and oil/gas production areas are possible notable contributors to the GOM dry deposition measurements collected in the Four Corners area.

Keywords

Air Pollution; Arid Area; Gaseous Oxidized Mercury; Dry Deposition; Surrogate Surface Passive Sampling

1. Introduction

Atmospheric mercury affects the globe (Lindberg et al., 2007; Slemr et al., 2003) and is a neurotoxicant that can negatively affect human health and aquatic regimes (Lyman et al., 2019; Bernhoft, 2012). Deposition of atmospheric mercury occurs through both wet and dry processes. Extended length mercury wet deposition measurements are ongoing in North America (National Atmospheric Deposition Program, 2019; Weiss-Penzias et al., 2016; Prestbo and Gay, 2009), but there is a current scarcity of extended length mercury dry deposition measurement studies.

Atmospheric mercury consists of gaseous elemental mercury (GEM), gaseous oxidized mercury (GOM), and particle bound mercury (PBM). GEM is largely insoluble and inert with long atmospheric lifetimes and can be transported globally, while GOM has a shorter atmospheric lifetime and is associated with local/regional mercury emission sources (Skov et al., 2007; Schroeder and Munthe, 1998). GOM can also form through higher temperature and photochemical activity (e.g. ozone) induced oxidation of GEM (Lin et al., 2012). GOM comprises a notable amount of total mercury dry deposition (Lyman et al., 2019; Lin et al., 2012) and, similar to PBM, deposits more readily to water, soil, and plants than GEM (Zhang et al., 2009). Surrogate surface measurement of GOM dry deposition using cation exchange membranes has been previously evaluated (Gustin et al., 2015; Huang et al., 2011; Lai et al., 2011; Lyman et al., 2009) and is useful in tracking seasonal and spatial variations of GOM dry deposition (Wright et al., 2014; Sather et al., 2014; Sather et al., 2013; Huang et al., 2012). These cation exchange membranes have been produced to specifically collect GOM as opposed to GEM or PBM (Wright et al., 2016). There is a need for additional

reliable measurements of GOM and PBM, and surrogate surface passive sampling could help meet this need in a more cost effective and simple to use and deploy manner (Pirrone et al., 2013).

The Four Corners area of the southwestern U.S.A. comprises the land where the states of New Mexico, Colorado, Utah, and Arizona meet (Figure 1). This area contains oil/gas production basins in northwestern New Mexico and southwestern Colorado (collectively known as the San Juan Basin) and in southeastern Utah (Paradox Basin), along with two of the largest coal-fired power plants in the U.S.A. (the Four Corners and San Juan power plants, pictured in the lower panel of Figure 1 along with the smaller regional power plants Nucla and Escalante). Coal-fired power plants comprise the highest anthropogenic mercury emission source in the U.S.A. at an estimated 50% mercury emissions contribution (U.S. EPA, 2012). Due to implementation of the Mercury and Air Toxics Standards (MATS) rule (U.S. EPA, 2012), mercury emissions were generally reduced 90% from large power plants across the U.S.A. (U.S. EPA, 2012) during the time period 2012-2016. According to estimates from the EPA's Toxic Release Inventory (TRI), annual emissions of mercury compounds to the air at the Four Corners power plant decreased by 97% from 488 lbs (221 kg) in 2009 to 14 lbs (6 kg) in 2018 (U.S. EPA, 2020a). Most of this decrease occurred after the closure of three units at the Four Corners power plant by December 31, 2013, resulting in a 78% decrease from 394 lbs (179 kg) of mercury released to the air in 2013 to 88 lbs (40 kg) of mercury in 2014. The San Juan power plant had previously reduced its mercury emissions from 2007-2009, going from 430 lbs (195 kg) of mercury in 2007 to 193 lbs (88 kg) of mercury in 2008 to 49 lbs (22 kg) of mercury in 2009. For 2018 the San Juan power plant reported an even lower release of 2 lbs (1 kg) of mercury.

Given the large mercury emission reductions from regional power plants in the U.S.A. due to implementation of the national MATS rule, this study investigated whether or not GOM dry deposition in the Four Corners area exhibited statistically significant decreased levels during the August, 2017-August, 2019 time period as compared to the earlier sampling period from August, 2009-August, 2011 which preceded many of the mercury reductions (Sather et al., 2013). The hypothesis that change had occurred between the two periods was tested against the alternative that no change had occurred (i.e., a two-sided hypothesis test). The authors believe that this is the first paper comparing pre-MATS rule and post-MATS rule measurement results from extended length GOM dry deposition studies using surrogate surface passive samplers. A comparison study using the continuous Tekran instrument showed evidence of reduced ambient mercury concentrations after implementation of the MATS rule in Maryland, U.S.A. (Castro and Sherwell, 2015).

2. Materials and Methods

2.1 Sampling sites

As seen in Figure 1, GOM dry deposition was sampled from August, 2017-August, 2019 at the same six locations which gathered GOM dry deposition measurements earlier from August, 2009-August, 2011 (Sather et al., 2013). Budgetary constraints forced the closure of the Farmington Airport site after one year. Each site is identified by its name and National Acid Deposition Program (NADP) code. The Molas Pass site (CO96) is a high elevation and

complex terrain remote mountain site which is only impacted by regional and global anthropogenic mercury emissions. Local anthropogenic mercury sources negligibly affect site CO96 but do impact the five remaining sites: Mesa Verde National Park – CO99, Valles Caldera National Preserve – NM97, Navajo Lake – NM98, Farmington Airport – NM99, and Farmington Substation – NM95. Monitoring site details, including elevation, latitude/longitude, and meteorological data are found in Table 1.

2.2 Field data collection

Smooth-edge surrogate surface passive sampling was again used to sample GOM dry deposition during contiguous two-week integrated time periods from August 1, 2017-August 1, 2019. Some samples were longer than two weeks (i.e., three, four or six weeks) due to the U.S. government shutdown at the end of 2018 and beginning of 2019, and because bad weather made some sites inaccessible at times. The use of surrogate surface passive sampling, including use of the smooth-edge surrogate surface passive sampler, has been a common and previously tested sampling method for measuring GOM dry deposition (Huang and Gustin, 2015; Castro et al., 2012; Gustin et al., 2012; Peterson et al., 2012; Peterson and Gustin, 2008; Lyman et al., 2009; Lyman et al., 2007). Passive sampling allows for GOM dry deposition measurements to be more easily collected in complex terrain remote high altitude locations, such as the Molas Pass site (CO96). This allows for the comparison of GOM dry deposition data from only regional and global anthropogenic mercury sources to data from other sites.

The Frontier Atmospheric Dry Deposition (FADD) device (Eurofins Frontier Global Sciences, Tacoma, Washington), developed earlier by scientists at the University of Nevada (Lyman et al., 2009; Peterson and Gustin, 2008), and shown to correlate with the Tekran continuous instrument in the earlier 2009-2011 Four Corners study (Sather et al., 2013), was again used to collect measurements of GOM dry deposition. ICE 450 negatively charged polysulfone impregnated cation exchange filter membranes from Pall Corporation mounted inverted into a polyurethane aerodynamic filter holder at about 3 meters above ground level were used in the previous study (Sather et al., 2013), but a switch to the Mustang S polyethersulfone membranes, also made by Pall Corporation, was necessary because the ICE 450 membranes are no longer manufactured. The University of Nevada, Reno has successfully used the Mustang S membranes in surrogate surface passive sampling of GOM dry deposition (Huang and Gustin, 2015), and this study conducted a collocated comparison between ICE 450 and Mustang S membranes at site NM95 before deploying Mustang S membranes to all of the study sites. At site NM95 the Mustang S membrane agreed well with the ICE 450 membrane with similar measured GOM dry deposition estimates and a Pearson correlation coefficient of 0.9 (Figure S1).

Hourly meteorological data were measured at four of the six sites (Figure 1). The meteorological data were gathered by the National Park Service for the Mesa Verde National Park (CO99) and Valles Caldera National Preserve (NM97) sites, and by the New Mexico Environment Department for the Farmington Substation (NM95) and Navajo Lake (NM98) sites. One-week integrated wet mercury deposition measurements were gathered at two of

the six sites (Figure 1) as part of the ongoing national NADP Mercury Deposition Network (MDN).

Although hourly meteorological data were not collected at the Molas Pass site (CO96), NADP rain gage data were available from the Molas Pass site as part of the data collected from the ongoing NADP MDN.

2.3 Laboratory procedures

All samples were prepared and shipped to the field sites in the same fashion as in the earlier 2009-2011 Four Corners study (Sather et al., 2013). All samples were then chemically analyzed at Eurofins Frontier Global Sciences in the same fashion as in the earlier 2009-2011 Four Corners study (Sather et al., 2013) using cold vapor atomic fluorescence spectroscopy (CVAFS) following Eurofins Frontier Global Sciences Standard Operating Procedure (SOP) FGS-069, U.S. EPA Method 1631 revision E (U.S. EPA, 2002) and additional quality assurance procedures for mercury analysis (Brown et al., 2011; Pandey et al., 2011). The detection limit for the surrogate surface FADD device was calculated as three times the standard deviation of the field blanks.

2.4 Statistical analyses

As done for the earlier 2009-2011 study (Sather et al., 2013), the precision for the study was obtained through evaluation of the relative percent difference (RPD) values for all valid FADD filter membrane field sample duplicates. GOM dry deposition estimates were compared both within sites between the August, 2009-August, 2011 and August, 2017-August, 2019 time frames and between sites within each time period. In addition, comparison was made between the first and second halves of ten year wet deposition records at two sites. Many of the distributions were skewed toward the upper end and due to the outlying values and non-normality, comparisons of median values were made with the nonparametric Wilcoxon rank sum test and the magnitudes of the differences calculated by Hodges-Lehmann estimates (See Hollander et al. (2013) for discussion of these procedures and Table S1 for summary data used in the Wilcoxon and Hodges-Lehmann analyses.).

Differences in variances can affect the significance levels resulting from the Wilcoxon testing. In addition, dispersion of the observations within sites between the two time periods was of interest itself. The equality of variances between the time periods was assessed using Miller’s jackknife procedure (Miller, 1968; Hollander et al., 2013). In comparisons of variances using smaller sample sizes and with distributions nearer to normality, the folded F statistic was used (SAS, 2012). The effect of different variances on the Wilcoxon test was investigated by van der Vaart (1961) and extended by Pratt (1964) to develop adjustment factors for the resulting p-values and these were used here, when needed. Spearman correlation coefficients were calculated between wet and dry deposition at two sites. All statistical procedures were implemented in SAS (2012).

2.5 Wind back trajectory analyses

To obtain suggested mercury emission source impacts on the Four Corners area monitoring sites, wind back trajectory analyses were again conducted for the highest three and lowest

three GOM dry deposition two-week sampling periods at Mesa Verde National Park (CO99) for the two-year period August, 2017-August, 2019; CO99 recorded the highest GOM dry deposition rate. This same analysis was conducted for site CO99 for the two-year period August, 2009-August, 2011 (Sather et al., 2013). As before, the National Oceanic and Atmospheric Administration (NOAA) HYSPLIT model was used in the analyses (NOAA, 2019).

3. Results and Discussion

3.1 Detection limit and precision of surrogate surface passive sampling

The detection limit and precision quality assurance results for the 2017-2019 study were similar to those from the earlier 2009-2011 study (Table 2). The median RPD over the 3-week, 4-week, and 6-week field sample duplicates was also 10%.

3.2 Analyses of GOM dry deposition measurement data

3.2.1 Site-to-site comparisons within the 2017-2019 and 2009-2011 GOM dry deposition data.—

Table S2 presents the results of comparing the measured samples from each site to all the other sites within both the 2009-2011 and 2017-2019 data sets. The table reports the results of the Wilcoxon rank sum test (as adjusted by the Pratt method, if needed) with Hodges-Lehmann estimates (ng/m^2) indicating the magnitude of the differences of median values as A – B, where A – B is the site pair at the left column of the table. One observes that the results were very similar between the time periods with respect to site-to-site comparisons; that is, site pairs which were significantly different from each other in 2009-2011 were also (almost always) different in 2017-2019. (Recall, however, that all results for NM99 (Farmington Airport) are qualified by the fact that the site was discontinued in October, 2018.) Another salient feature from Table S2 is that CO96 (Molas Pass) received significantly lower GOM dry deposition than any other site during both sampling periods, providing support for site CO96 as only being affected by regional and global mercury emission sources with no, or negligible, local mercury emission impact. Note that the differences in median values between site CO96 and all the other sites increased in the 2017-2019 dataset and all differences were statistically significant at the 1% confidence level. Conversely, CO99 (Mesa Verde National Park) received significantly higher GOM dry deposition during both periods than any other site, excepting NM95 (Farmington Substation) in 2017-2019. Also, the table indicates that during both time frames NM95 (Farmington Substation) saw higher GOM dry deposition than did NM98 (Navajo Lake) to its east.

3.2.2 Within site comparisons of 2017-2019 data with 2009-2011 data.—

Analysis of the four years of GOM dry deposition data (excluding NM99) collected in the Four Corners area suggests a decrease in GOM dry deposition estimates at the high elevation remote mountain site (Molas Pass - CO96) from 2009-2011 to 2017-2019, and an increase in GOM dry deposition estimates at the remaining four study sites from 2009-2011 to 2017-2019 (Figure 2, Table 3, Table S1). Table 3 reports the mean and standard deviation of the GOM dry deposition rate estimates and the GOM dry deposition totals for each site for both two-year sampling periods. From Table 3, a 25% decrease in the mean GOM dry

deposition rate estimate between August, 2009-August, 2011 and August, 2017-August, 2019 was measured for the Molas Pass site (CO96), while increases in mean GOM dry deposition rate estimates ranging from 14% to 33% between August, 2009-August, 2011 and August, 2017-August, 2019 were measured at the four other sites.

As seen in the 2009-2011 data there continued to be a strong regional signature in the GOM dry deposition data set for 2017-2019, with the highest GOM dry deposition estimates again recorded during the spring and summer across the Four Corners area at the five non-remote sites (Figure S2). Note in Figure S2, though, that the high elevation remote mountain site CO96 (Molas Pass) did not record a large increase in measured GOM dry deposition during the spring and summer months of 2018, unlike the increases at the other five measurement sites. Also, site CO96 actually recorded lower GOM dry deposition estimates during the spring and summer months of 2019 when the other sites were again recording large GOM dry deposition estimate increases. These observations reinforce the idea that site CO96 is negligibly affected by local anthropogenic mercury emission sources compared to the other five measurement sites. Table S3 reports comparisons of the spring-summer (April-September) median values versus the fall-winter (October-March) median values. As seen there, the warmer season was statistically significantly higher at CO99 (Mesa Verde National Park), NM95 (Farmington Substation), and NM98 (Navajo Lake). The difference between spring-summer and fall-winter median values at site CO96 was only 13 ng/m^2 (not statistically significantly different).

As noted above, the measurements at the Molas Pass high elevation remote mountain site (CO96) with its complex terrain suggest that it is dominated by regional, national and global anthropogenic mercury sources with no significant local mercury emission source contribution. However, the five remaining study sites are likely also affected by local anthropogenic mercury emission sources from nearby cities and oil/gas production areas. It is suggested that the U.S.A. regional/national MATS power plant mercury emission decreases (90% control on large power plants) are largely driving the GOM dry deposition decrease seen at the Molas Pass site because: (1) recent publications indicate that overall global emissions of mercury have increased (Streets et al., 2019; UN Environment, 2019), and (2) despite the impact of nearby large regional wildfires in year 3 of the study in the Four Corners area (i.e., the Durango 416 and Burro wildfires in June-July, 2018), GOM dry deposition did not increase at the Molas Pass site in 2017-2019 versus 2009-2011, but indeed decreased (Table 3, Table 4). Figure 3 displays the time series for each of the four years of GOM dry deposition sampling at the Molas Pass site (CO96). The highest 2-week GOM dry deposition values occurred in year 3 during the large regional Durango 416 and Burro wildfires in June and July of 2018 which were near the Molas Pass site. The lowest 2-week GOM dry deposition values occurred in year 4 during the spring and summer of 2019. (Table S4 also reports a statistically significantly lower median GOM dry deposition level at CO96 in year 4.) Focusing on the data for the three months from the first part of April to the first part of July for all four sampling years (the time series data within the oval in Figure 3), it was noted that the total amount of precipitation collected in the NADP rain gage at site CO96 was 3.25 inches (8.26 cm) in year 1, 8.76 inches (22.3 cm) in year 2, 2.94 inches (7.47 cm) in year 3, and 8.15 inches (20.7 cm) in year 4. Higher precipitation amounts in year 4 (20.7 cm) likely contributed to the lower GOM dry deposition measured at Molas

Pass (i.e., 406 ng/m^2 from April 9, 2019 to July 2, 2019), but the U.S.A. regional MATS mercury emission reductions probably also contributed to the lower GOM dry deposition measured at Molas Pass in year 4 of the study because the similar high precipitation amount recorded in year 2 (22.3 cm) before full implementation of MATS coincided with much higher GOM dry deposition measured at the Molas Pass site (i.e., 1001 ng/m^2 from April 12, 2011 to July 5, 2011).

At the remaining five sites, Figure 2 is suggestive of an increase in GOM dry deposition estimates measured in years 3 and 4 compared to years 1 and 2. Figure 2 also displays how different site CO96 is from the other five sites. Note from Figure 2 how site CO96 did not show an increase in annual GOM dry deposition means in either year 2 or year 3, and year 3 contained the large regional wildfires close to site CO96. It is suggested that site CO96 did not show an increase in GOM dry deposition in year 3 despite the impact of the nearby large regional wildfires because of the large regional power plant mercury emission reductions which effectively mitigated the GOM dry deposition increase from the wildfires, and because site CO96 is also not affected (or negligibly affected) by local anthropogenic mercury emissions.

Hotter temperatures (Table 1), higher ozone concentrations measured at nearby city monitoring sites (U.S. EPA Air Quality System (AQS) database), and the nearby large regional wildfires, all likely contributed to elevating GOM dry deposition levels at the five non-remote sites in year 3. Hotter temperatures and higher ozone concentrations measured at nearby city monitoring sites also contributed to the elevated GOM dry deposition levels at the five non-remote sites in year 2. However, despite the much lower ambient temperatures recorded in year 4 (Table 1), Figure 2 implies the GOM dry deposition recorded at four of those five sites (NM99 did not operate in year 4) was still higher than year 1 and similar to year 2 (similar to year 1 for site NM97). These temperature and photochemical observations suggest that local anthropogenic mercury emissions are notably contributing to the total GOM dry deposition being collected at these five non-remote sites, and also suggest that local anthropogenic mercury emissions have increased in the August, 2017-August, 2019 time period compared to the August, 2009-August, 2011 time period. Fugitive (non-stack) emissions of mercury, which presumably would be primarily released from local anthropogenic mercury sources, have increased in the U.S.A. since 2013 based on the national EPA TRI database (U.S. EPA, 2020b).

Indeed, at the highest GOM dry deposition study site, Mesa Verde National Park (CO99), Table 1 finds annual mean humidity, annual mean temperature, and annual total precipitation numbers were similar in study year 1 (8/09-8/10) and study year 4 (8/18-8/19), yet the mean 2-week GOM dry deposition estimate for study year 4 was 403 ng/m^2 compared to the mean 2-week GOM dry deposition estimate of 241 ng/m^2 for study year 1. At the Valles Caldera National Preserve site (NM97), the mean 2-week GOM dry deposition estimate for study year 4 was 192 ng/m^2, similar to the 170 ng/m^2 mean 2-week GOM dry deposition estimate for study year 1 under similar meteorological regimes between those two study years (Table 1).

Table 4 presents the results of comparing the GOM dry deposition median values between 2009-2011 and 2017-2019 at each site. As with the site-to-site comparisons, the Wilcoxon rank sum test was used (with the Pratt adjustment, if needed) and differences in ng/m^2 indicated by Hodges-Lehmann estimates, expressed as the difference 2017-2019 minus 2009-2011. Table 4 also reports for each site the results of Miller's jackknife comparison of the variances of the observations between each time period; the size of the dispersion differentials is reported as the 2017-2019 to 2009-2011 ratio of the standard deviations. The table reveals that the GOM dry deposition median value was lower in 2017-2019 than in 2009-2011 at CO96 (Molas Pass) by 17 ng/m^2 (Hodges-Lehmann estimate), but was higher at both CO99 (Mesa Verde National Park) and NM95 (Farmington Substation) by 66 ng/m^2 and 64 ng/m^2, respectively. Though increased levels were suggested, no statistically significant difference was detected at the other three sites: NM97 (Valles Caldera National Preserve), NM98 (Navajo Lake), or NM99 (Farmington Airport). Results at NM99 are qualified by the shortened sampling. The variance comparisons showed that the dispersion increased at each site except CO96 (Molas Pass) where no significant change was found. The increases in standard deviations at the five sites outside of Molas Pass ranged from just over 60% to almost double.

At Molas Pass (CO96), the results of the formal testing are consistent with the anticipated decrease in GOM dry deposition levels due to the reduced power plant mercury emissions. However, the statistically significant increases at Mesa Verde National Park (CO99) and Farmington Substation (NM95) are counterintuitive. These results suggest the influence of other factors at these sites (and possibly the other three where increases were estimated, but not outside the realm of random variability). The statistically significant increases in variability and their magnitudes found at every site except Molas Pass again strongly reinforces the idea that other factors (quite possibly multiple ones) are at play in the Four Corners area outside of Molas Pass.

Thus, after consideration of all of the results and detailed discussion presented above, it is suggested that local mercury emissions from nearby cities (i.e., from the Farmington and Durango MSAs near sites CO99, NM95, NM99 and NM98, and the Santa Fe/Los Alamos and Albuquerque MSAs near site NM97, all depicted by population density in Figure 1) are likely contributing GOM dry deposition at the five non-remote Four Corners area sites outside of Molas Pass. In addition, it is suggested that mercury emissions from any oil/gas combustion source in the San Juan Basin and Paradox Basin are contributing GOM dry deposition at sites CO99, NM95, NM99 and NM98 (Site NM97 is not located in either basin). Local anthropogenic mercury emission sources can include medical incineration, cremation, refineries, cement manufacturing, vehicular emissions, caustic soda production, metals manufacturing, and re-emission from soil disturbance (McLagan et al., 2018; Gworek et al., 2017; Cheng et al., 2017). Combustion occuring at an oil/gas production source also releases mercury emissions to the air (UN Environment, 2019; Gworek et al., 2017).

3.2.3 Comparison of wind back trajectory analyses at Mesa Verde National Park site.—

As done in Sather et al. (2013) on the 2009-2011 baseline study, wind back trajectories were constructed for the three highest and three lowest GOM dry deposition two-week sampling periods at the Mesa Verde National Park site (CO99) from August,

2017-August, 2019, the site which again consistently produced the highest GOM dry deposition estimates for the Four Corners area. From August, 2017-August, 2019 the highest two-week GOM dry deposition estimate of 1316 ng/m^2 at the Mesa Verde National Park site (CO99) was measured from June 20 – July 3, 2018 (Figure 4). The National Oceanic and Atmospheric Administration (NOAA) HYSPLIT model (NOAA, 2019) was used to construct six 48-hour wind back trajectories and one 24-hour wind back trajectory for the June 20-July 3, 2018 time period. In contrast to the highest GOM dry deposition estimate two-week period from the 2009-2011 baseline study (March 29-April 12, 2011), none of the June 20-July 3, 2018 wind back trajectories passed over the two largest Four Corners area power plants. Instead, the wind back trajectories passed over a nearby city (Durango, Colorado) and the Durango 416, Burro wildfire area (for the 7/3 trajectory), or nearby oil/gas production areas in southwestern Colorado and southeastern Utah (for the 7/3 and 6/27 trajectories). This provides support that regional wildfire and local mercury emission sources were contributing to the highest GOM dry deposition estimates measured at the Mesa Verde National Park site. The wind back trajectory maps for the second and third highest GOM dry deposition two-week sampling periods at site CO99 for the 2017-2019 study similarly show arriving air masses passing over nearby city areas or oil/gas production areas in southwestern Colorado, northwestern New Mexico and southeastern Utah, instead of over the Four Corners and San Juan power plants (Figures S3 and S4). In Figures S3 and S4 the trajectories also trace back to the large Phoenix, Arizona metropolitan area. No precipitation was recorded at the Mesa Verde National Park site on any of the three highest two-week sampling periods.

As in the previous 2009-2011 baseline study, wind back trajectories were also produced for the three lowest GOM dry deposition two-week sampling periods at the Mesa Verde National Park site (CO99). Similar to the back trajectories produced in the 2009-2011 baseline study, the lowest three two-week sampling periods for 2017-2019 had back trajectories passing through mercury emission sources such as power plants, cities and oil/gas production areas, but significant precipitation was recorded during all three two-week sampling periods (Figures S5–S7).

3.2.4 Collocated Dry and Wet Deposition Mercury Data results at sites CO96 and CO99.—

Two study sites, CO96 and CO99, also collected weekly collocated wet deposition mercury measurements as part of the U.S.A. NADP program for all four years of this study. The NADP data were matched to the two-week dry deposition sampling periods to obtain total mercury deposition estimates. For the wet deposition data, NADP assigns quality ratings to the samples, and only “A” and “B” codes are designated as valid; this criterion was also applied here. No significant Spearman correlation coefficients were observed between the wet and dry deposition. Analysis of all two-week periods during the four years which contained valid and collocated GOM dry deposition and total mercury wet deposition data revealed the following study year by study year GOM dry deposition percentages of the total mercury deposition estimates: For CO96 (Molas Pass): 27% for study year 1, 20% for study year 2, 21% for study year 3, and 14% for study year 4. For CO99 (Mesa Verde National Park): 30% for study year 1, 48% for study year 2, 65% for study year 3, and 62% for study year 4. Over the two-year time frames, the GOM dry

deposition fractions were: 23% for 2009-2011 and 17% for 2017-2019 at Molas Pass; 37% for 2009-2011 and 63% for 2017-2019 at Mesa Verde. Table S4 presents the comparison of dry, wet, and total deposition between years 3 and 4. The only statistically significant differences were that GOM dry deposition (median values) were lower in year 4 at CO96 (Molas Pass) and at NM97 (Valles Caldera National Preserve).

The NADP mercury wet deposition data were aggregated on a twelve-month basis beginning with 2009, the first year of collection at CO96, with scaling of each total wet deposition value by the corresponding precipitation amount (Figures S8 and S9). The resulting ten year time series for 2009-2019 for both CO96 and CO99 were analyzed via the exact Wilcoxon rank sum test comparing the first five years to the latter five. The end of the first five years extended just past the final implementation of the mercury controls at the Four Corners Power Plant. This analysis showed a significant (at the 10% level) decrease in the measured mercury wet deposition at both sites. The Hodges-Lehmann estimates of the declines between the five-year periods were 52 ng/m^2 per inch of precipitation at Molas Pass and 232 ng/m^2 per inch of precipitation at Mesa Verde National Park. Scaling the wet deposition values by the precipitation amounts removes the effect of differing amounts of precipitation, and these results provide a robust comparison of the wet deposition data collected before and after the major mercury emission reductions from the Four Corners power plant and also before and after the final national MATS rule compliance date of April, 2016. Total mercury wet deposition contains both wet deposition of GOM and PBM. It is suggested that total wet mercury deposition has declined at the Mesa Verde National Park site because ambient fine particle concentrations have also declined at the site. Though fine particle data are not collected at the Molas Pass site, fine particle ambient concentrations as reported in the EPA's AQS database at the Mesa Verde National Park site (CO99) decreased 27% for $PM_{2.5}$ from a 2009-2011 average of 3 ug/m^3 to a 2017-2018 average of 2.2 ug/m^3, and decreased 35% for PM10 from a 2009-2011 average of 7.4 ug/m^3 to a 2017-2018 average of 4.8 ug/m^3.

4. Conclusions

This study in the Four Corners area provides the first comparison in the U.S.A. of pre-MATS rule and post-MATS rule measurement results from extended length GOM dry deposition monitoring campaigns using surrogate surface passive samplers. On an annual basis, dry mercury deposition (represented in this study by GOM dry deposition measurements) ranges from 30%-65% of total mercury deposition at the Mesa Verde National Park site and ranges from 14%-27% at the high elevation remote Molas Pass mountain site based upon four years of collocated GOM dry deposition and total mercury wet deposition measurements. *A priori*, one might suppose that the significant mercury emission reductions from the large local and regional power plants in the U.S.A. due to implementation of the national MATS rule would result in decreases in measured GOM dry deposition at all sites in the Four Corners area during the August, 2017-August, 2019 time period. However, the two-sided hypothesis testing done here found a statistically significant decrease at just one site and statistically significant increases at two others.

A statistically significant measured decrease in GOM dry deposition was documented at Molas Pass (CO96), a complex terrain high elevation mountain site only affected by regional

and global anthropogenic mercury emissions. Since recent publications indicate overall global anthropogenic mercury emissions inventory estimates have increased and since local anthropogenic mercury emissions at Molas Pass would be considered negligible, it is suggested that regional mercury emission reductions from large power plants across the U.S.A., especially from the Four Corners and San Juan power plants, accounted for the statistically significant decrease in GOM dry deposition measured at the Molas Pass high elevation remote mountain site.

At the remaining five sites, two (CO99 – Mesa Verde National Park and NM95 – Farmington Substation) exhibited statistically significant increases in GOM dry deposition while the other three sites (NM98 – Navajo Lake, NM97 – Valles Caldera National Preserve, and NM99 – Farmington Airport) recorded statistically nonsignificant GOM dry deposition increases. Unlike Molas Pass, these sites are not as remote, and it is suggested that local mercury emissions from nearby cities and oil/gas production areas in southeast Utah, southwest Colorado and northwest New Mexico, are contributing to GOM dry deposition at these five sites. Additionally, higher GOM dry deposition estimates occurred at all of the Four Corners area sites during the large regional wildfires in June and July, 2018 close to Durango, Colorado (i.e., the Durango 416 and Burro wildfire complex); this suggests the importance of occasional large wildfires to GOM dry deposition loading in affected ecosystems.

This study produced data helpful to assessing the effectiveness of the U.S.A. national MATS rule in reducing large concentrated mercury emission plumes from large coal-fired power plants across the U.S.A. GOM dry deposition data collected with surrogate surface passive samplers can be used as a credible indicator of anthropogenic mercury emissions from both large concentrated regional sources, such as large coal-fired power plants, as well as nearby local anthropogenic mercury emissions from city and oil/gas production area sources. It is recommended that additional GOM dry deposition data be taken in the future in the Four Corners area to assess the effectiveness of further reducing mercury emissions from the remaining large power plant units in the area, and to gather additional data to further study the contribution of local mercury emission sources which appear to notably influence GOM dry deposition in the Four Corners area.

Supplementary Material

Refer to Web version on PubMed Central for supplementary material.

Acknowledgements and Disclaimer

The authors are grateful to the following managers and field operators involved in careful ambient data collection, including Roman Szkoda and Kara Lopez of the New Mexico Environment Department, Kelly Palmer and Robert Brantlinger of the U.S. Forest Service (USFS)/Bureau of Land Management (BLM), Paul Bohmann and Andrew Spear of the National Park Service (NPS-Mesa Verde National Park), and Robert Parmenter and Scott Compton of the Valles Caldera National Preserve. From Eurofins Frontier Global Sciences, Robert Brunette and Jeanne Harrel provided outstanding work on project and data management. The authors are also grateful to Diana Greiner, Eric Nystrom and Stephen Angle of the U.S. EPA Region 6 for their detailed GIS map work, to Amy Mager of the NADP for furnishing the wet deposition data, and to Ethan Brown of the U.S. EPA Region 8 for overall project collaboration. The U.S. EPA through its Office of Research and Development funded and managed the research described here under contract number EP-W-13-024 to Serco, Inc as a part of the Regional Applied Research Effort (RARE) program. This paper has been subjected to Agency review and approved for publication.

References

Bernhoft RA, 2012. Mercury toxicity and treatment: a review of the literature, Journal of Environmental Public Health, 2012.

Brown RJC, Kumar Y, Brown AS, Kim K-H, 2011. Memory Effects on Adsorption Tubes for Mercury Vapor Measurement in Ambient Air: Elucidation, Quantification, and Strategies for Mitigation of Analytical Bias, Environmental Science & Technology, 45, 7812–7818. [PubMed: 21842877]

Castro MS and Sherwell J, 2015. Effectiveness of Emission Controls to Reduce the Atmospheric Concentrations of Mercury, Environmental Science & Technology, 49, 14000–14007. [PubMed: 26606506]

Castro MS, Moore C, Sherwell J, Brooks SB, 2012. Dry deposition of gaseous oxidized mercury in Western Maryland, Science of the Total Environment, 417-418, 232–240.

Cheng I, Zhang L, Castro M, Mao H, 2017. Identifying Changes in Source Regions Impacting Speciated Atmospheric Mercury at a Rural Site in the Eastern United States, Journal of the Atmospheric Sciences, 74, 2937–2947.

Gustin MS, Amos HM, Huang J, Miller MB, Heidecorn K, 2015. Measuring and modeling mercury in the atmosphere: a critical review, Atmospheric Chemistry and Physics, 15, 5697–5713.

Gustin MS, Weiss-Penzias PS, Peterson C, 2012. Investigating sources of gaseous oxidized mercury in dry deposition at three sites across Florida, USA, Atmospheric Chemistry and Physics, 12, 9201–9219.

Gworek B, Dmuchowski W, Baczewska AH, Bragoszewska P, Bemowska-Kalabun O, Wrzosek-Jakubowska J, 2017. Air Contamination by Mercury, Emissions and Transformations – A Review, Water, Air and Soil Pollution, 228: 123.

Hollander M, Wolfe DA, Chicken E 2013. Nonparametric Statistical Methods. John Wiley & Sons, New York, 848 pp.

Huang J, Choi H-D, Landis MS, Holsen TM, 2012. An application of passive samplers to understand atmospheric mercury concentration and dry deposition spatial distributions, Journal of Environmental Monitoring, 14(11), 2976–2982. [PubMed: 23001454]

Huang J, Liu Y, Holsen TM, 2011. Comparison between knife-edge and frisbee-shaped surrogate surfaces for making dry deposition measurements: Wind tunnel experiments and computational fluid dynamics (CFD) modeling, Atmospheric Environment, 45, 4213–4219.

Huang J and Gustin MS, 2015. Use of Passive Sampling Methods and Models to Understand Sources of Mercury Deposition to High Elevation Sites in the Western United States, Environmental Science & Technology, 49, 432–441. [PubMed: 25485926]

Lai S-O, Huang J, Hopke PK, Holsen TM, 2011. An evaluation of direct measurement techniques for mercury dry deposition, Science of the Total Environment, 409, 1320–1327.

Lin C-J, Shetty SK, Pan L, Pongprueksa P, Jang C, Chu H-W, 2012. Source attribution for mercury deposition in the contiguous United States: Regional difference and seasonal variation, Journal of the Air & Waste Management Association, 62(1), 52–63. [PubMed: 22393810]

Lindberg S, Bullock R, Ebinghaus R, Engstrom D, Feng X, Fitzgerald W, Pirrone N, Prestbo E, Seigneur C, 2007. A Synthesis of Progress and Uncertainties in Attributing the Sources of Mercury in Deposition, Ambio, 36, 19–32. [PubMed: 17408188]

Lyman SN, Cheng I, Gratz LE, Weiss-Penzias P, Zhang L, 2019. An updated review of atmospheric mercury, Science of the Total Environment, 707, 135575.

Lyman SN, Gustin MS, Prestbo EM, Kilner PI, Edgerton E, Hartsell B, 2009. Testing and Application of Surrogate Surfaces for Understanding Potential Gaseous Oxidized Mercury Dry Deposition, Environmental Science & Technology, 43, 6235–6241. [PubMed: 19746719]

Lyman SN, Gustin MS, Prestbo EM, Marsik FJ, 2007. Estimation of Dry Deposition of Atmospheric Mercury in Nevada by Direct and Indirect Methods, Environmental Science & Technology, 41, 1970–1976. [PubMed: 17410792]

McLagan DS, Hussain BA, Huang H, Lei YD, Wania F, Mitchell CPJ, 2018. Identifying and evaluating urban mercury emission sources through passive sampler-based mapping of atmospheric concentrations, Environmental Research Letters, 13, 074008.

Miller RG Jr. 1968. Jackknifing variances, Annals of Mathematical Statistics. 39, 567–582.

National Atmospheric Deposition Program, 2019. National Atmospheric Deposition Program 2018 Annual Summary. Wisconsin State Laboratory of Hygiene, University of Wisconsin-Madison, WI.

NOAA (National Oceanic and Atmospheric Administration), 2019. HYSPLIT (Hybrid Single-Particle Lagrangian Integrated Trajectory) Model access via NOAA ARL READY Website (http://ready.arl.noaa.gov/HYSPLIT.php). NOAA Air Resources Laboratory, Silver Spring, MD.

Pandey S, Kim K-H, Brown RJC, 2011. Measurement techniques for mercury species in ambient air, Trends in Analytical Chemistry, 30(6), 899–917.

Peterson C and Gustin M, 2008. Mercury in the air, water and biota at the Great Salt Lake (Utah, USA), Science of the Total Environment, 405, 255–268.

Peterson C, Alishahi M, Gustin MS, 2012. Testing the use of passive sampling systems for understanding air mercury concentrations and dry deposition across Florida, USA, Science of the Total Environment, 424, 297–307.

Pirrone N, Aas W, Cinnirella S, Ebinghaus R, Hedgecock IM, Pacyna J, Sprovieri F, Sunderland EM, 2013. Toward the next generation of air quality monitoring: Mercury, Atmospheric Environment, 80, 599–611.

Pratt JW, 1964. Robustness of some procedures for the two-sample location problem, Journal of the American Statistical Association, 59, 665–680.

Prestbo EM and Gay DA, 2009. Wet deposition of mercury in the U.S. and Canada, 1996-2005: Results and analysis of the NADP mercury deposition network (MDN), Atmospheric Environment, 43, 4223–4233.

SAS, 2012. SAS OnlineDoc® 9.3, SAS Institute, Cary, NC.

Sather ME, Mukerjee S, Allen KL, Smith L, Mathew J, Jackson C, Callison R, Scrapper L, Hathcoat A, Adam J, Keese D, Ketcher P, Brunette R, Karlstrom J, Van der Jagt G, 2014. Gaseous Oxidized Mercury Dry Deposition Measurements in the Southwestern USA: A Comparison between Texas, Eastern Oklahoma, and the Four Corners Area, The Scientific World Journal, 2014, 580723. [PubMed: 24955412]

Sather ME, Mukerjee S, Smith L, Mathew J, Jackson C, Callison R, Scrapper L, Hathcoat A, Adam J, Keese D, Ketcher P, Brunette R, Karlstrom J, Van der Jagt G, 2013. Gaseous oxidized mercury dry deposition measurements in the Four Corners area and Eastern Oklahoma, U.S.A., Atmospheric Pollution Research, 4, 168–180.

Schroeder WH and Munthe J, 1998. Atmospheric Mercury – An Overview, Atmospheric Environment, 32, 809–822.

Skov H, Sorensen BT, Landis MS, Johnson MS, Sacco P, Goodsite ME, Lohse C, Christiansen KS, 2007. Performance of a new diffusive sampler for Hg^0 determination in the troposphere, Environmental Chemistry, 4, 75–80.

Slemr F, Brunke E-G, Ebinghaus R, Temme C, Munthe J, Wangberg I, Schroeder W, Steffen A, Berg T, 2003. Worldwide trend of atmospheric mercury since 1977, Geophysical Research Letters, 30, 1516, 4 pp.

Streets DG, Horowitz HM, Lu Z, Levin L, Thackray CP, Sundland EM, 2019. Global and regional trends in mercury emissions and concentrations, 2010-2015, Atmospheric Environment, 201, 417–427.

UN Environment, 2019. Global Mercury Assessment 2018. UN Environment Programme, Chemicals and Health Branch, Geneva, Switzerland. Available online at: https://www.unenvironment.org/resources/publication/global-mercury-assessment-2018

U.S. EPA AQS database. Available online at: http://www.epa.gov/aqs

U.S. EPA, 2020a. Toxics Release Inventory (TRI). Available online at: http://www.epa.gov/trinationalanalysis/introduction-2018-tri-national-analysis

U.S. EPA, 2020b. Toxics Release Inventory (TRI). Available online at: http://www.epa.gov/trinationalanalysis/mercurv-air-releases-trend

U.S. EPA, 2012. Final Mercury and Air Toxics Standards (MATS) rule available at 77 Federal Register 9304 (dated February 16, 2012) and online at: http://www.gpo.gov/fdsys/pkg/FR-2012-02-16/pdf/2012-806.pdf Rule summary material also available online at: http://www.epa.gov/mats/cleaner-power-plants

U.S. EPA, 2002. Method 1631, Revision E: Mercury in Water by Oxidation, Purge and Trap, and Cold Vapor Atomic Fluorescence Spectrometry, EPA-821-R-02-019, August, 2002. Available at: http://water.epa.gov/scitech/methods/cwa/metals/mercury/upload/2007_07_10_methods_method_mercury_1631.pdf

van der Vaart HR, 1961. On the robustness of Wilcoxon's two-sample test, in Quantitative Methods in Pharmacology, de Jonge H (ed.), Interscience, New York, pp. 140–158.

Weiss-Penzias PS, Gay DA, Brigham ME, Parsons MT, Gustin MS, ter Schure A, 2016. Trends in mercury wet deposition and mercury air concentrations across the U.S. and Canada, Science of the Total Environment, 568, 546–556.

Wright G, Gustin MS, Weiss-Penzias P, Miller MB, 2014. Investigation of mercury deposition and potential sources at six sites from the Pacific Coast to the Great Basin, USA, Science of the Total Environment, 470-471, 1099–1113.

Wright LP, Zhang L, Marsik FJ, 2016. Overview of mercury dry deposition, litterfall, and throughfall studies, Atmospheric Chemistry and Physics, 16, 13399–13416.

Zhang L, Wright LP, Blanchard P, 2009. A review of current knowledge concerning dry deposition of atmospheric mercury, Atmospheric Environment, 43, 5853–5864.

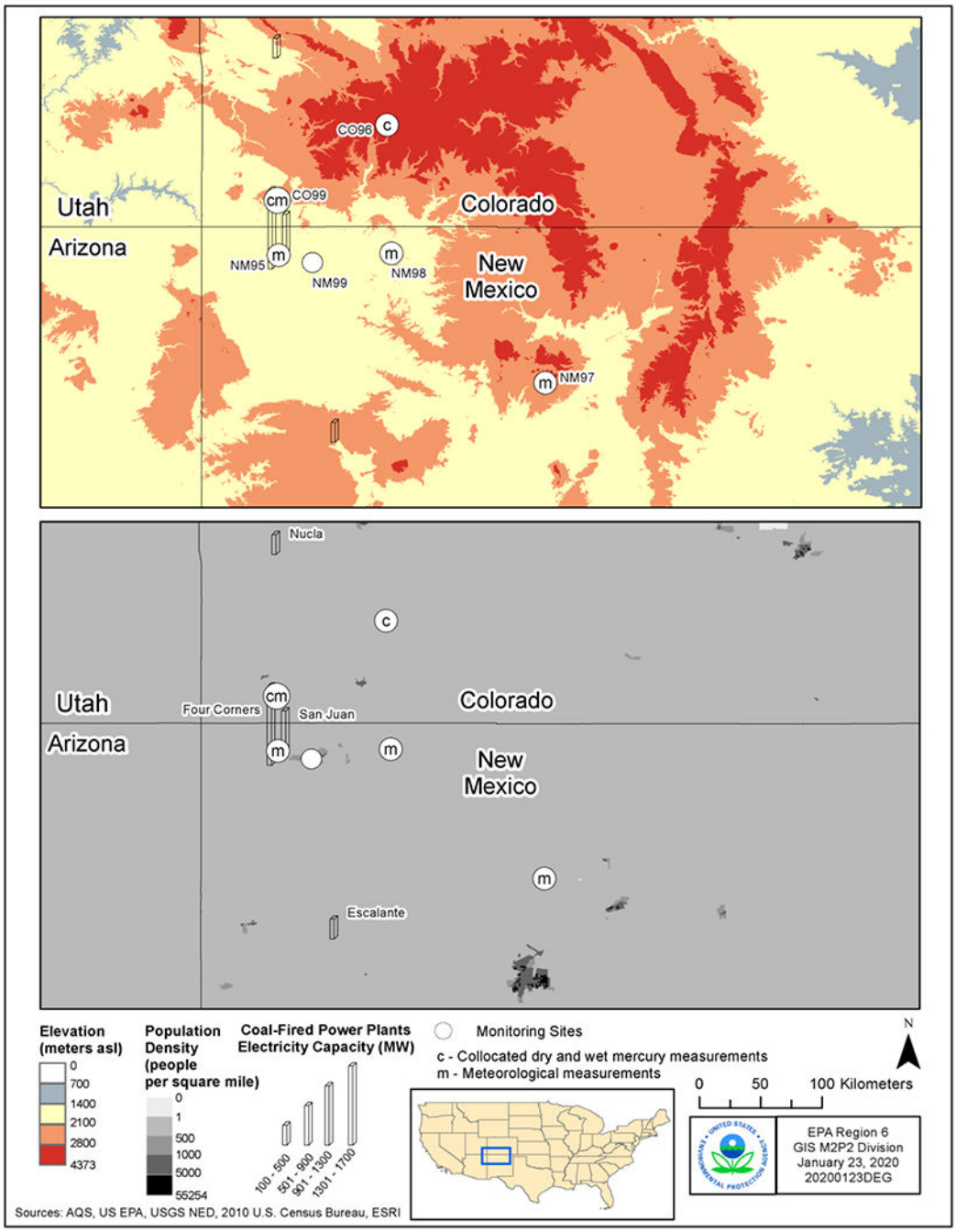

Figure 1.

Monitoring sites for the August, 2017-August, 2019 Four Corners Area GOM Dry Deposition Monitoring Study.

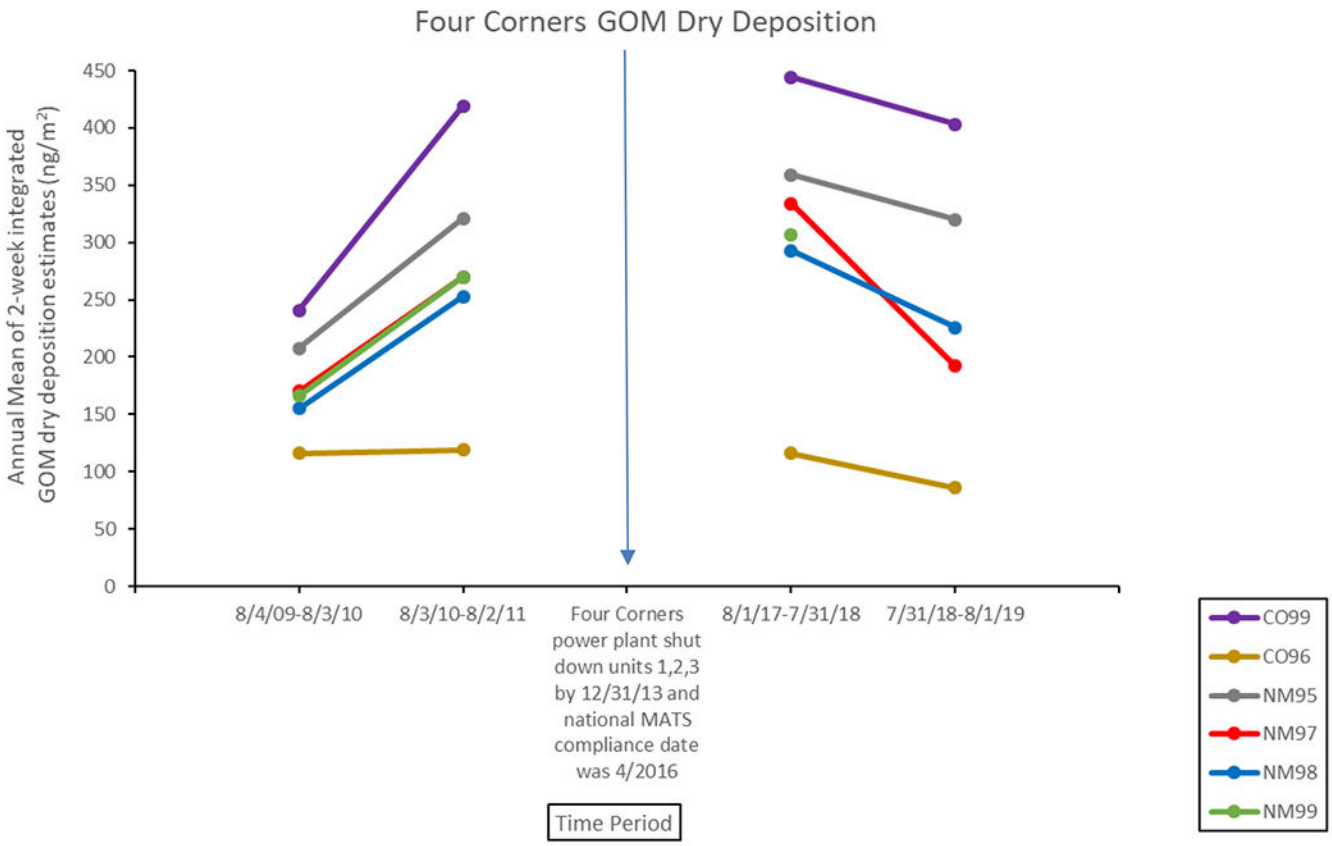

Figure 2.

Mean two-week GOM dry deposition data at all 6 Four Corners Area sites for 2009-2011 and 2017-2019 studies.

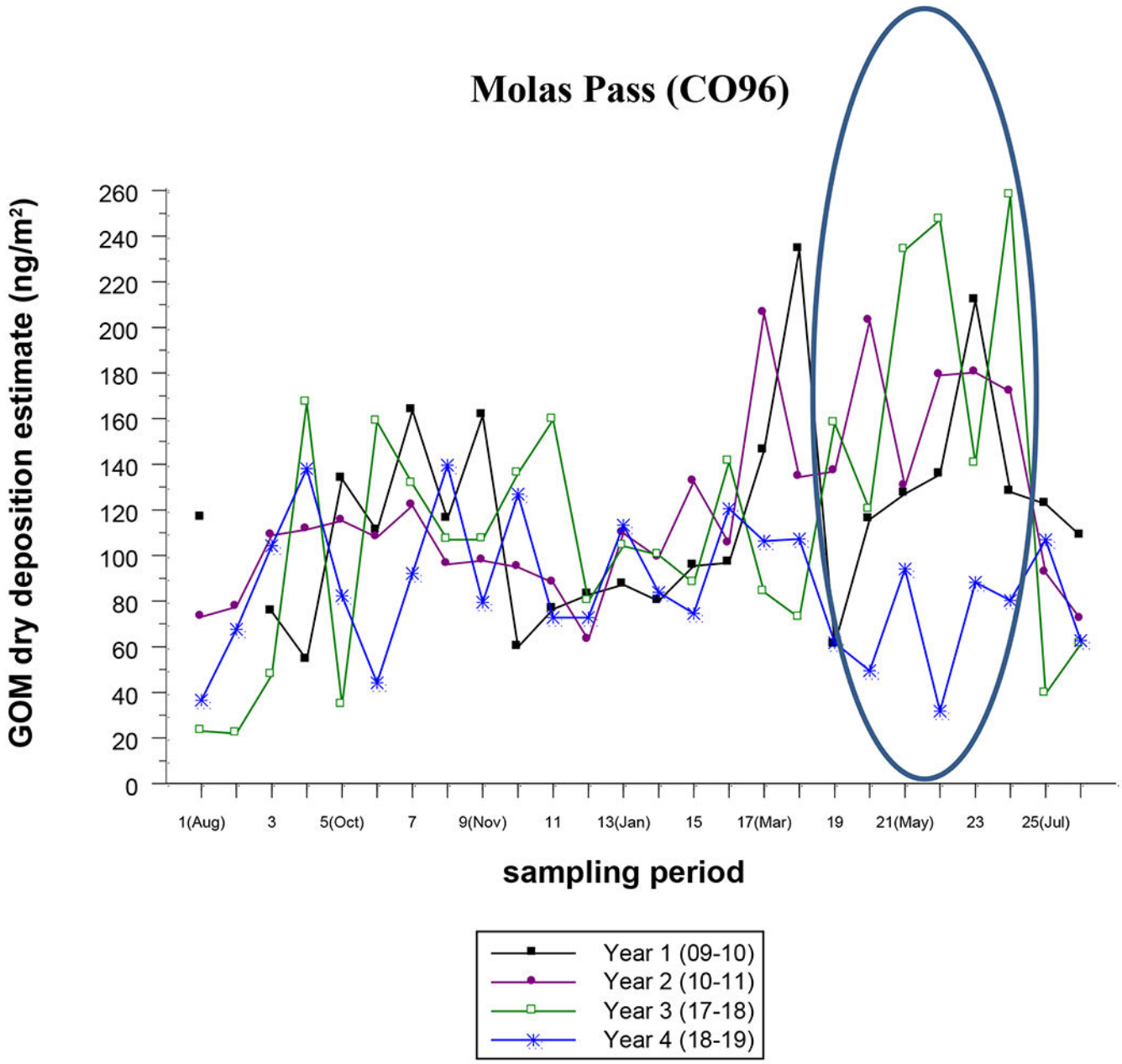

Figure 3.
GOM dry deposition data time series for all four study years at the Molas Pass site (CO96).

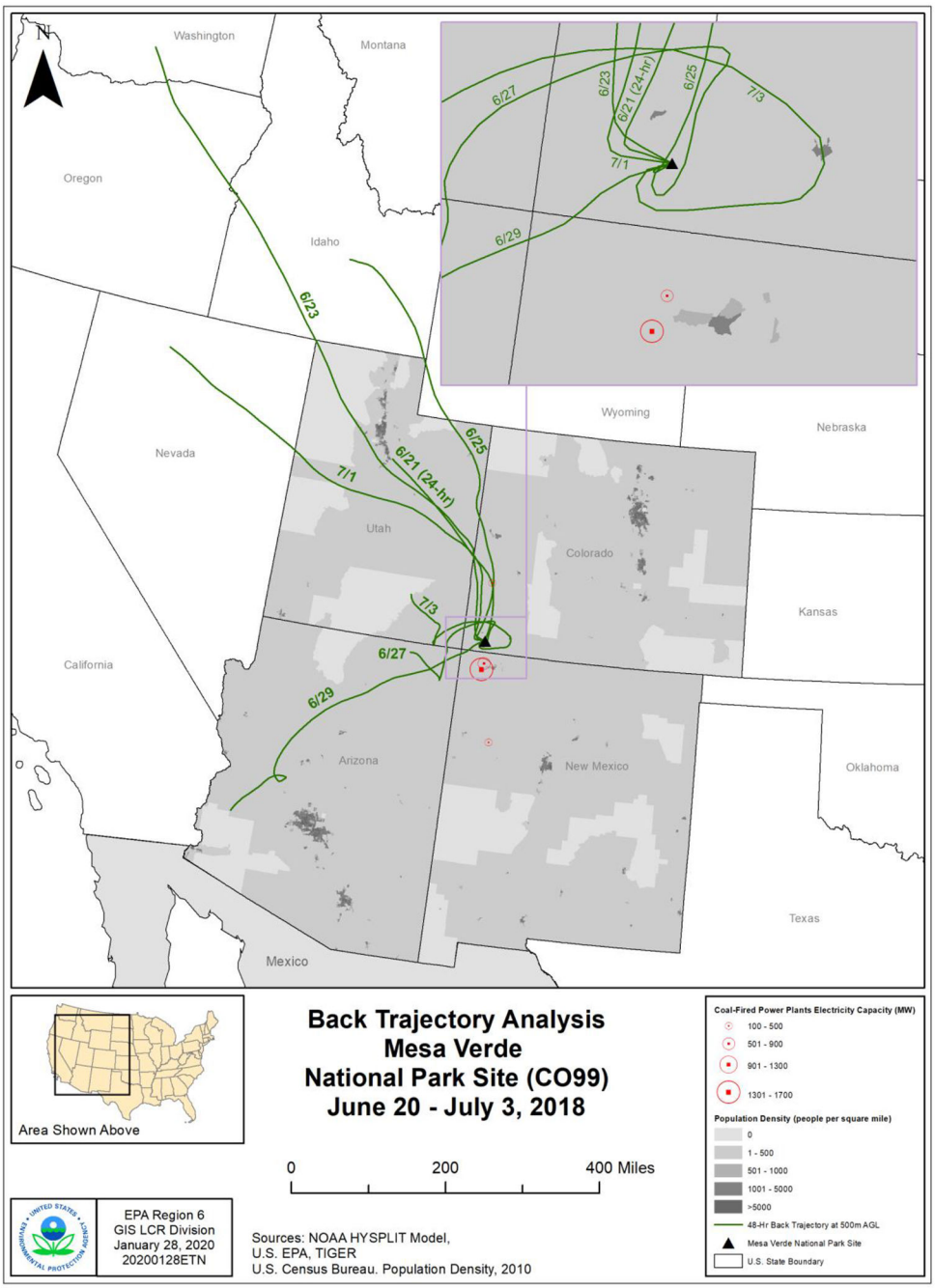

Figure 4.

Back trajectory analysis for the Mesa Verde National Park site (CO99) for June 20 – July 3, 2018. Seven contiguous 48-hour back trajectories ending at 1000 LST on July 3, 2018 (except for June 20-21 which is a 24-hour back trajectory). End date of each 48-hour back trajectory plotted for each trajectory trace (e.g. 7/3 represents 48-hour back trajectory for 7/1 – 7/3); Four Corners area coal-fired power plant locations are located at the center of the open circles.

Table 1.

Four Corners area GOM dry deposition monitoring sites location and meteorological characteristics: Year 1 = August 4, 2009 – August 3, 2010; Year 2 = August 3, 2010 – August 2, 2011; Year 3 = August 1, 2017 – July 31, 2018; Year 4 = July 31, 2018 – August 1, 2019; asl = above sea level; dec. = decimal; deg. = degrees; F = fahrenheit.

Site	Elevation	Latitude	Longitude	Annual Humidity means (%)				Annual Temperature means (deg. F)				Annual Precipitation totals (inches)			
	meters asl	Dec. deg.	Dec. deg.	Year 1	Year 2	Year 3	Year 4	Year 1	Year 2	Year 3	Year 4	Year 1	Year 2	Year 3	Year 4
Mesa Verde National Park (CO99)	2172	37.1981	−108.4903	44	43	35	48	48.8 (9.3 deg. C)	50.5 (10.3 deg. C)	53.3 (11.8 deg. C)	49 (9.4 deg. C)	14.38 (365 mm)	14.49 (368 mm)	8.13 (207 mm)	17.9 (455 mm)
Farmington Substation (NM95)	1678	36.797625	−108.480153	na	na	na	na	52.4 (11.3 deg. C)	54.3 (12.4 deg. C)	57.9 (14.4 deg. C)	54 (12.2 deg. C)	na	na	na	na
Farmington Airport (NM99)	1674	36.737467	−108.23369	na	na	na	na	na	na	na	na	na	na	na	na
Valles Caldera National Preserve (NM97)	2657	35.8584	−106.5214	61	53	47	59	38.5 (3.6 deg. C)	42.1 (5.6 deg. C)	44.7 (7.1 deg. C)	40.9 (4.9 deg. C)	21.96 (558 mm)	16.13 (410 mm)	19.07 (484 mm)	24.6 (625 mm)
Navajo Lake (NM98)	1972	36.8097	−107.6515	na	na	na	na	48.4 (9.1 deg. C)	50 (10 deg. C)	52.3 (11.3 deg. C)	49.9 (9.9 deg. C)	na	na	na	na
Molas Pass (CO96)	3249	37.7514	−107.6853	na	na	na	na	na	na	na	na	na	na	na	na

Table 2.

Detection limit and precision quality assurance results for 2009-2011 and 2017-2019 Four Corners GOM dry deposition studies.

Study Time Period	Detection Limit (ng/filter)	Average field blank (ng/filter)	Median RPD	Percent field duplicates <= 20% RPD
2009-2011	0.42	0.3	10%	78%
2017-2019	0.33	0.14	10%	71%

Table 3.

Two year GOM dry deposition (dep.) estimates for Four Corners area sites; August 4, 2009-August 2, 2011 study and August 1, 2017-August 1, 2019 study; h=hour.

Site	Mean surrogate surface dep. rate estimate (ng/m^2h) ± standard deviation 2009-2011 study	Mean surrogate surface dep. rate estimate (ng/m^2h) ± standard deviation 2017-2019 study	GOM dry dep. estimate cumulative total (ng/m^2) 2009-2011 study	GOM dry dep. estimate cumulative total (ng/m^2) 2017-2019 study
Mesa Verde National Park (CO99)	1.0 ± 0.6	1.3 ± 1.0	17155	22016
Farmington Substation (NM95)	0.8 ± 0.5	1.0 ± 0.8	13738	17653
Valles Caldera National Preserve (NM97)	0.7 ± 0.4	0.8 ± 0.6	10653	13694
Navajo Lake (NM98)	0.6 ± 0.4	0.8 ± 0.6	10609	13489
Molas Pass (CO96)	0.4 ± 0.1	0.3 ± 0.1	6007	5258

Table 4.

Within site comparisons of the median values and variances between the August, 2009-August, 2011 and August, 2017-August, 2019 sampling periods.[a] Units for differences are ng/m^2 Ratios of standard deviations are (2017-2019)/(2009-2011).[b].

Site	(2017-2019)–(2009-2011)	Std. dev. ratio
CO96	−17**	1.27
CO99	66*	1.70**
NM95	64*	1.92***
NM97	21	1.67**
NM98	42	1.63**
NM99[c]	45	1.97***

[a]: Comparisons used Wilcoxon's rank sum test with Pratt's adjustment, when needed. Magnitude of differences are Hodges-Lehmann estimates.

[b]: Variance comparisons done with Miller's jackknife testing.

[c]: NM99 (Farmington Airport) terminated after first year.

***: significant at the 1% level.

**: significant at 5% level.

*: significant at 10% level.